Separation Harmonics to Discern Broken Bar Fault from Load Torque Oscillation in Three Phase Induction Motor

Taner Goktas, Muslum Arkan*

Abstract— This paper presents separation harmonics to discriminate rotor failure from low frequency load torque oscillations in three phase induction motors. The most common method for detecting broken rotor bar faults is to analyze the corresponding sidebands through motor current signature analysis (MCSA). If a motor is subjected to load fluctuation, then the oscillation related sidebands exhibit similar behaviors as well. Particularly, when the load fluctuation frequency is close or equal to that of broken bars, the stator current spectrum analysis can be misleading. In this study, torque and motor phase voltage waveforms are exhaustively analyzed to discriminate broken rotor bar fault from low frequency load torque oscillation in three phase induction motors. In order to extract and justify the separation patterns, 2-D Time Stepping Finite Element Method (TSFEM) is used. The simulation and experimental results show that the proposed approach can successfully be applied to fault separation process in star connected motors.

Index Terms— Broken rotor bar, fault diagnosis, Finite Element, load torque oscillation, MCSA method, phase voltage, torque spectrum

1 INTRODUCTION

IN induction machines are highly preferred due to their cost advantage, robustness, and high power capabilities. Fault diagnosis, failure prognosis and condition monitoring of these machines are critical to avoid costly unscheduled operation interrupts. Motor current signature analysis is the most widely used method for condition monitoring which employs frequency spectrum of phase currents. Among all fault types, broken rotor bar faults account for 5%-10% of failures reported for induction motors [1]. In the case of broken rotor bar failure, additional harmonics appear as the sidebands of fundamental harmonic. For induction motor running under constant load, these harmonics are defined in (1) by using MCSA [2].

$$f_b = \left(\left(\frac{k}{p} \right)(1-s) \pm s \right) f_s \qquad \frac{k}{p} = 1, 5, 7, \ldots \tag{1}$$

where k is the harmonic index and p is the number of pole pairs. The harmonics at $(1\pm2s)f_s$ are the most commonly used harmonics to detect broken rotor bar failure. The amplitudes of these sideband harmonics depend on rotor inertia, load level and the severity of rotor fault. The sideband harmonics distance to the fundamental harmonic is proportional to the motor slip as depicted in Fig. 1. Sometimes, these harmonics appear even in a healthy induction motor spectrum due to manufacturing imperfections. In healthy case, they usually have smaller amplitude than broken rotor bar fault case.

Intensive research has been conducted to detect broken rotor bar faults under constant load conditions. In [3], broken rotor bar fault at different relative bar positions is observed through Finite Element Model (FEM).

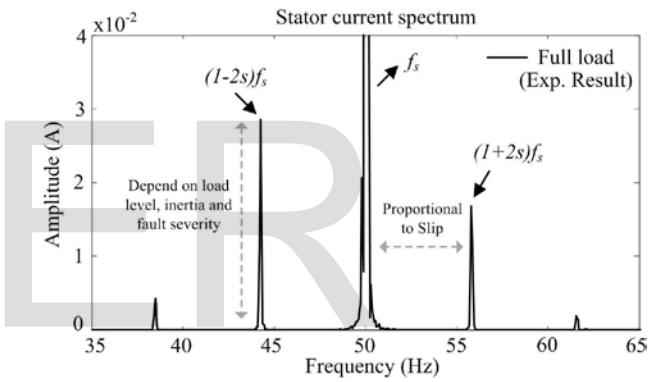

Fig. 1. The sidebands harmonics, broken rotor bar fault

In [4], the components around the space harmonics in the current spectrum are analyzed to detect broken rotor bar fault. It is pointed out that some broken bar signatures around the third, fifth and seventh current harmonics are observed. The generated torque fluctuates due to these current harmonics, especially the sixth harmonic in torque spectrum can be observed when there are fifth and seventh harmonics in the current spectrum. A novel frequency pattern during the start-up period [5], and Shannon wavelets [6] are used to detect fault in induction motors. However, to achieve an accurate and comprehensive detection process, the load conditions should also be taken into account.

In a system experiencing load torque oscillations, the sideband components at fs±fosc raise in stator phase current spectrum, where fosc represent load torque oscillation frequency. The oscillation related harmonics may sometimes overlap with broken rotor bar related (1) harmonics. Especially, if the load torque oscillation frequency is equal to broken rotor bar fault frequency, oscillation and broken rotor bar related harmonics can appear at the same spot on stator phase current spectrum. Therefore, the reflections of load oscillation on current spectrum should carefully be decomposed. Over the years, several papers addressing similar problems have been published in the litera-

• *Authors are with Inonu University, Department of Electric-Electronic Engineering, 44280, Malatya, Turkey.*
**Corresponding Author E- Mail: muslum.arkan@inonu.edu.tr*

ture [7-21]. In [7, 8], the separation of broken bar fault and load torque oscillation is achieved based on the measuring magnetic flux linked by one stator tooth. It is shown that the load torque oscillations have the same affect on the magnetic poles whereas broken bar faults affect the length of magnetic poles. In [9], to discern broken bar and load oscillation effects Vienna Monitoring Method (VMM) which can calculate flux linkage space phasor and electromagnetic torque is deployed. Using VMM a new fault index based on the difference of instantaneous voltage (t_v) and current torque (t_i) mathematical models is introduced [9]. In [10], components created by space harmonics are used to differentiate broken rotor failures and load torque oscillations. Instantaneous active and reactive powers [11], instantaneous active and reactive currents [12], are also suggested for the same purpose. It is shown that the load torque oscillation affects the instantaneous active components whereas the broken bar failures mainly affect the instantaneous reactive components [11], [12]. From instantaneous active and reactive power theory, active and reactive Park's vectors are developed to discern these two effects [13]. Phase displacement between space vector components [14-16], a combined analysis of the amplitude and phase spectra of the instantaneous active and reactive powers [17, 18], real and imaginary part of stator impedance [19], and the sidebands of inherent eccentricity signatures [20] are suggested for broken rotor bar fault detection during load torque oscillation. By using instantaneous power factor and phase angle, broken rotor bar failures, load torque oscillation and eccentricity failures are detected in [21].

In this study, separation harmonics are presented to discriminate broken bar failure from low frequency load torque oscillation in three phase line-fed star connected induction motor. Instead of analyzing phase current, torque and motor phase voltage spectrums are analyzed by using 2-D Finite Element Method (FEM). The theoretical findings are verified through experimental results.

2 Modelling Motor and Separation Harmonics

2.1 Modelling Induction Motor with 2-D FEM

The Finite Element Method (FEM) can be used to get approximate solutions in a pre-defined boundary. Thus, in order to model electric motor, ANSYS Maxwell 2-D interactive software package is used. Through the transient solver, this software can analyse magnetic fields, power, torque, speed, and flux of a model at various time steps of a solution over a specified period of time [22]. The variables are updated based on a time dependent motion equation component in the z-direction:

$$\nabla \times \upsilon \nabla \times A = J_s - \sigma \frac{dA}{dt} - \sigma \nabla V + \nabla \times H_c \qquad (2)$$

where H_c is the coercivity of the permanent magnet, A is the magnetic vector potential, V is the electric potential, υ is the reluctivity, J_s is the source of current density. The equation, (2) is executed in each time step at every node of FEM model. In order to minimize eddy current effects, stranded conductors are used in each winding. The filaments in each stranded winding are connected in series or parallel with different several locations. The current in each filament are the same and defined as:

$$\nabla \times \upsilon \nabla \times A = J_s \qquad (3)$$

Thus, the voltage in the winding terminal is as follows:

$$u_s = J_s \iint \frac{dA}{dt} . d\Omega + R . i_f + L . \frac{di_f}{dt} \qquad (4)$$

where R, L and if are the winding resistor, inductance, and winding current, respectively. In order to obtain comparative simulation and experimental results, the detailed stator/rotor structure and parameters of the test motor are used in the simulations. Electrical and mechanical parameters of the motor are given in Table. I.

TABLE 1
PARAMETERS OF THE TEST MOTOR

Number of poles	4
Outer diameter of stator, *mm*	145
Inner diameter of stator, *mm*	89
Outer diameter of rotor, *mm*	88
Inner diameter of rotor, *mm*	34.7
Number of stator slots, *mm*	36
Number of rotor bars	28
Rated voltage, *V*	400
Rated frequency, *Hz*	50
Rated power, *kW*	2.2
Rated current, *A*	4.7
Rotor inertia, *kgm2*	0.047

The simulation model shown in Fig. 2 is designed based on the actual size and geometry of all parts, such as stator core, rotor core, shaft, rotor bar structure. Furthermore, stator winding configuration, air gap, physical conditions of the stator conductors, stator and rotor magnetic material are also taken into account. To create one broken bar condition, the corresponding bar is modelled as three times less conductivity than the rest bars so that the eddy currents can be taken into account in the broken bar. Fig. 2., shows the magnetic flux density and flux distribution in healthy case, two broken bars case and load oscillation cases. As it can be seen in Fig 2a. (healthy), and Fig 2c. (load oscillation), the flux density distribution is symmetrical whereas the flux density distribution in Fig. 2b, is not symmetrical, particularly around the broken bars. It means that when the rotor bar is broken, the adjacent bars draw higher current than other bars [23-25].

Fig. 3 shows the radial flux density, Br, in one mechanical cycle at the same rotor position. It is shown in Fig 3b. that around the broken bars radial flux density reduces whereas around the adjacent bars it increases. During the load torque oscillation, there is no noticeable difference between healthy and oscillation cases in the air gap radial flux density (Fig. 3c). The reflections of this load oscillation on the current spectrum

may sometimes be misinterpreted due to commonalities between the broken bar signatures.

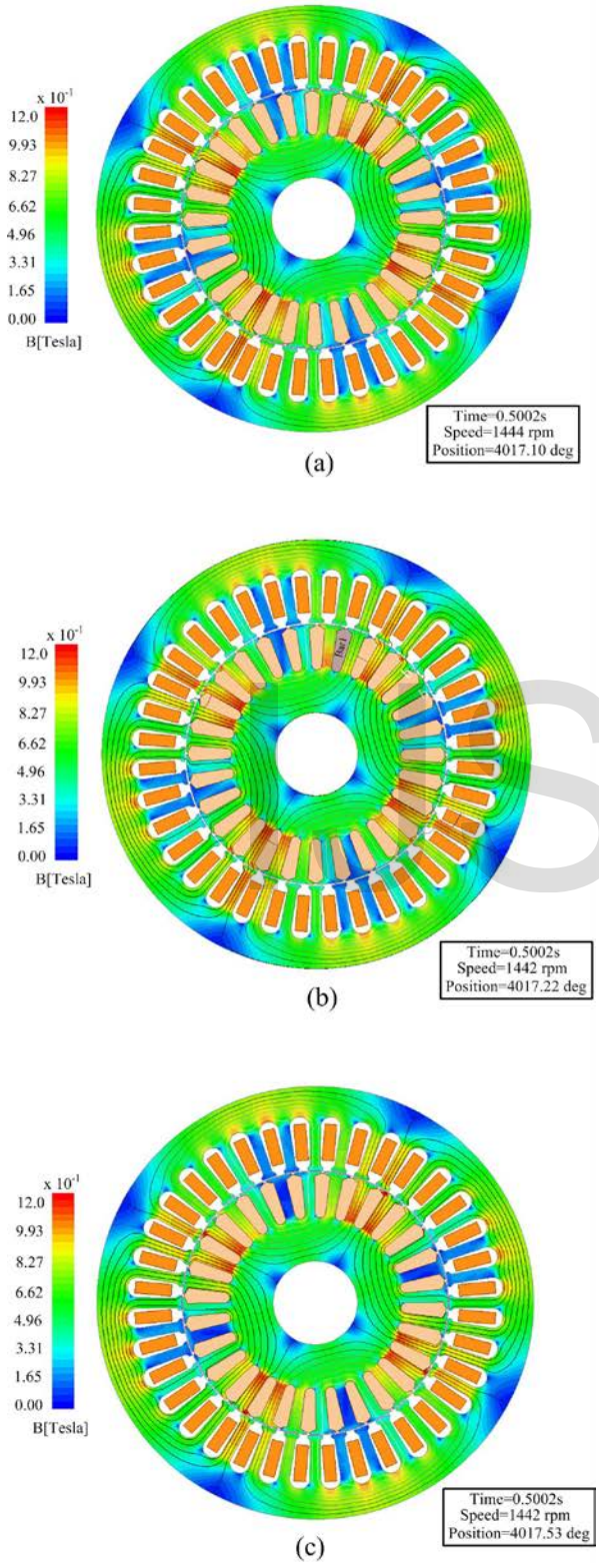

Fig. 2. Magnetic flux density and flux line distribution
a) Healthy motor b) Motor with broken bar c) Motor with load oscillation

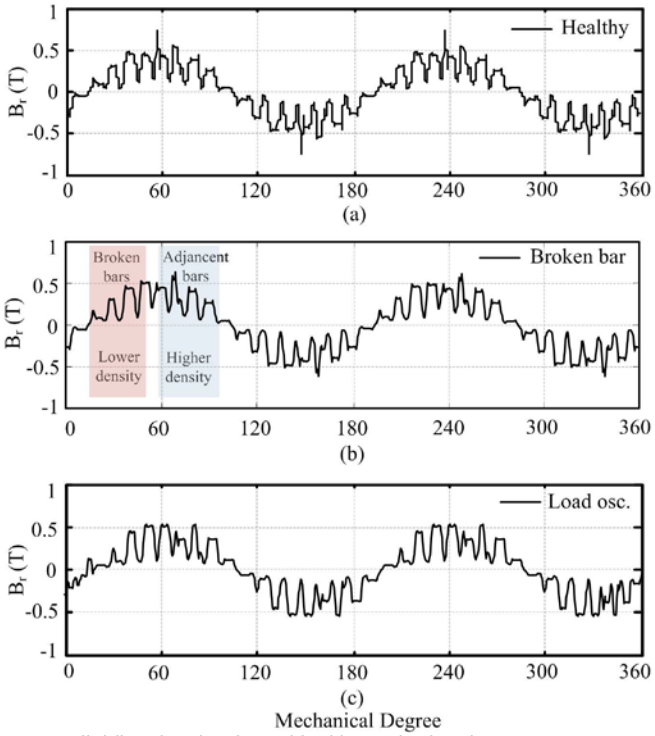

Fig. 3. Radial flux density a) Healthy b) Two broken bars
c) Load oscillation

2.3 Separation Harmonics

Under normal condition, there is only one magnetic field which rotates clockwise at sf_s frequency in the rotor. When a bar breaks, rotor currents produce a counter rotating magnetic field at $-sf_s$. This counter-clockwise magnetic field component creates a current component at $(1-2s)f_s$ frequency in the stator. Due to this stator component, torque and speed ripples are generated at $2sf_s$ frequency. These ripples produce two additional components: $(1-2s)f_s$ and $(1+2s)f_s$ on the stator side. As a result of this, broken bar can be detected simply by analysing sideband components at $(1\pm2s)f_s$ frequency on the current spectrum.

In the presence of load fluctuation, harmonics at fs±fosc appear on the stator current spectrum. The amplitude of these harmonics depends on peak value of oscillation, motor load and inertia. There are three types of load torque oscillation in induction motors: position-varying, single frequency and periodic load torque dip [16]. In this paper, single frequency load torque oscillation affecting current spectrum similar to broken rotor bar fault is investigated. Single frequency load torque oscillation can be modelled as in (5) [26]:

$$T_{load} = T_{avg} + T_{osc}\cos\left(2\pi f_{osc} t\right) \quad (5)$$

where T_{avg} is average torque, T_{osc} is oscillating torque and fosc is oscillating frequency. If T_{osc} and f_{osc} are smaller than average torque and supply frequency, harmonics at $f_s \pm f_{osc}$ appear in the stator phase current spectrum. When the oscillation frequency fosc increases, the effect of T_{osc} on the shaft and stator current decreases.

It is well-known that torque monitoring has been used for broken bar fault detection. When there is broken bar fault, the generated torque oscillates at a specific frequency close to dc component as given in (6) [27]:

$$f_b = 2ksf_s, \quad k = 1,2,3,... \tag{6}$$

The amplitude of these harmonics depends on oscillating torque amplitude, T_{osc}. In [27], some harmonics introduced in the torque spectrum caused by broken bar fault when the motor is saturated. These harmonics are close to 300 Hz which is six times of supply frequency in line-fed induction motors. In the case of broken bar, harmonics at $2ksf_s$, which is close to dc component and $6f_s$-$2ksf_s$ which is the sideband harmonic of $6f_s$, appear in the torque spectrum [27]. When the torque spectrum is analysed at low frequency load torque oscillation, the harmonic f_{osc} appears, however; the sidebands of $6f_s$ ($6f_s$-kf_{osc}) don't. It is because the load or shaft torque is negligibly affected from load oscillation at higher frequencies. The inertia of motor suppresses the load oscillation at higher frequencies which is close to $6f_s$. In addition, 5th and 7th harmonics in the current spectrum produce 6th harmonics in the torque spectrum. Hence, when the sidebands of 5th and 7th harmonics are analysed, it is clearly observed that there are some broken bar related signatures around the 5th and 7th harmonics in current spectrum but load torque oscillation related harmonics are in noise level. Hence, it is possible to use the sidebands of $6f_s$ to separate broken bar faults from low frequency load torque oscillation in the torque spectrum. So, separation harmonics for torque spectrum are defined as;

$$\left.\begin{matrix} k_1\begin{pmatrix} 2sf_s \\ f_{osc} \end{pmatrix}; \\ 6f_s - k_2\begin{pmatrix} 2sf_s \\ f_{osc} \end{pmatrix}; \end{matrix}\right\} \Rightarrow \left\{\begin{matrix} k_1 = 1,2,... & (\textit{for broken, osc}) \\ k_2 = 1,2,4 & (\textit{for broken}) \\ k_2 = 0 & (\textit{for osc}) \end{matrix}\right\} \tag{7}$$

The separation harmonics defined in (7) contain two integer variable; k_1 and k_2. The first integer variable k1 points out the harmonics ($k_1 2sf_s$, $k_1 f_{osc}$) close to dc components in torque spectrum both in broken bar and torque oscillation cases. But, the second integer variable k_2 used to separate broken bar and load oscillation is related to sideband harmonics of $6f_s$. When there is broken bar failure, non-zero k_2 values represent the sideband harmonics of $6f_s$ ($6f_s$-$2sf_s$, $6f_s$-$4sf_s$, $6f_s$-$8sf_s$). Unlike broken bar failure, k_2 becomes zero under low frequency load torque oscillation, which means that there is no sideband harmonics of $6f_s$. As seen in (7), k_2 indicates the source of the fault in torque spectrum.

Another proposed option to separate broken bar fault from low frequency load torque oscillation is defining some particular patterns in motor phase voltage spectrum. For this purpose, the motor phase voltage is measured between stator neutral point and phase input in star connected motor.

The measurement scheme is given in Fig. 5 where the star point of stator has to be accessible to measure motor phase voltage. The measured voltage equation can be written as:

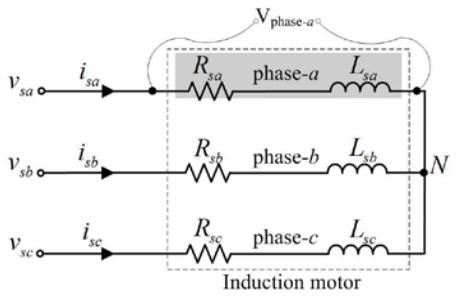

Fig. 4. Motor phase voltage, $v_{phase\text{-}a}$

$$v_{phase-a} = R_{sa} i_{sa} + \frac{d\psi_{sa}}{dt} \tag{8}$$

where i_{sa} is the stator current, R_{sa} is phase resistance and ψsa is the phase-a flux linkages. As shown in (8), the changes in phase current and linkage flux will be reflected to motor phase voltage. It is well known that if the system is perfectly balanced and there is no path for the third harmonic of current to flow, naturally the third harmonic and corresponding sidebands in the phase current are not observed. Since the phase current doesn't include any third harmonic in a balanced system, analysing the phase voltage spectrum or flux spectrum has the same meaning. Also, components around the third harmonics at flux $d\psi_{sa}/dt$ and voltage V_{phase_a} spectrums have the same amplitudes. When there is load torque oscillation, the system is still symmetrical (see Fig 2c. and Fig.3c) but has some additional harmonics in the flux and in the phase voltages. The system is becomes asymmetrical when bars are broken (see Fig 2b and Fig. 3b) and therefore some sidebands components pop-up around the third harmonic in the flux and voltage spectrums. In order to observe the effects of fault components, the motor phase voltage spectrum is analysed under broken bar and load torque oscillation cases. After several tests, it is concluded that the sidebands of 3rd harmonics don't have any load oscillation related harmonics though it has some broken bar fault related harmonics on the motor phase voltage spectrum. So, the separation harmonic for motor phase voltage is defined as;

$$\left.\begin{matrix} 3f_s - k_3\begin{pmatrix} 2sf_s \\ f_{osc} \end{pmatrix}; \end{matrix}\right\} \Rightarrow \left\{\begin{matrix} k_3 = 1,2 & (\textit{for broken}) \\ k_3 = 0 & (\textit{for osc}) \end{matrix}\right\} \tag{9}$$

As shown in (9), the sidebands of $3f_s$ in motor phase voltage spectrum are used for separation. The separation harmonics in (9) includes only one integer variable which is k_3. While the sideband harmonics $3f_s$-$2sf_s$ (k_3=1) and $3f_s$-$4sf_s$ (k_3=2) show up in the case of broken bar, there is only $3f_s$ (k_3=0) –but not the sidebands of $3f_s$– in low frequency load torque oscillation. Besides $3f_s$, the supply frequency harmonic f_s can be observed in the both cases. Thus, k_3 is considered as the key coefficient to discern broken rotor bar from low frequency load torque oscillation in motor phase voltage spectrum.

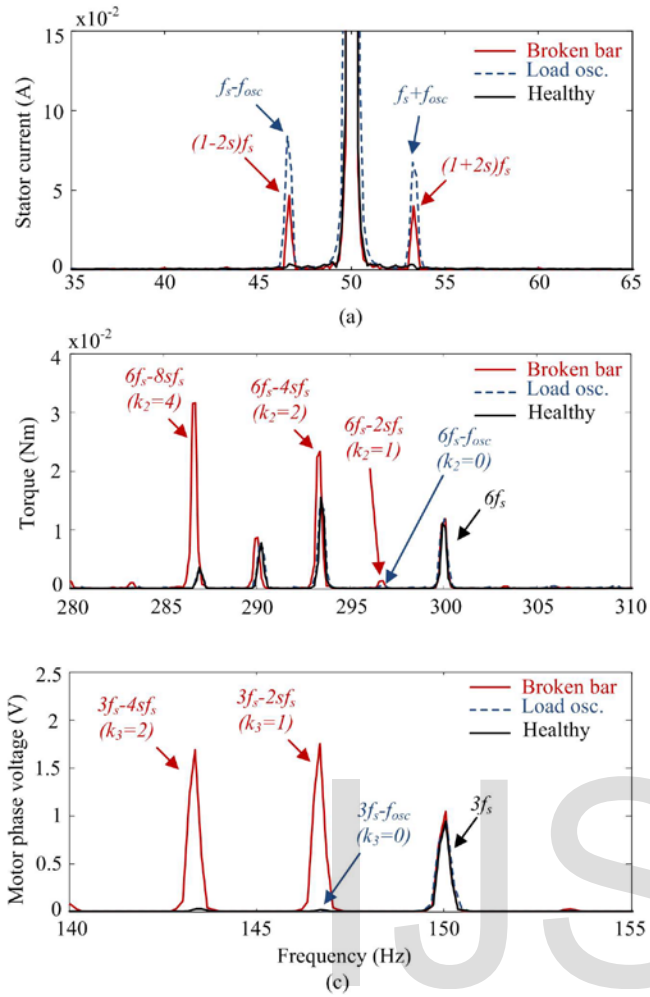

Fig. 5. Simulation results, 80% load, ($2sf_s = f_{osc}$=3.3 Hz) broken bar (solid line), load oscillation (dashed line)
a) Stator current spectrum (35- 65 Hz)
b) Torque spectrum (280- 310 Hz)
c) Motor phase voltage spectrum (140- 155 Hz)

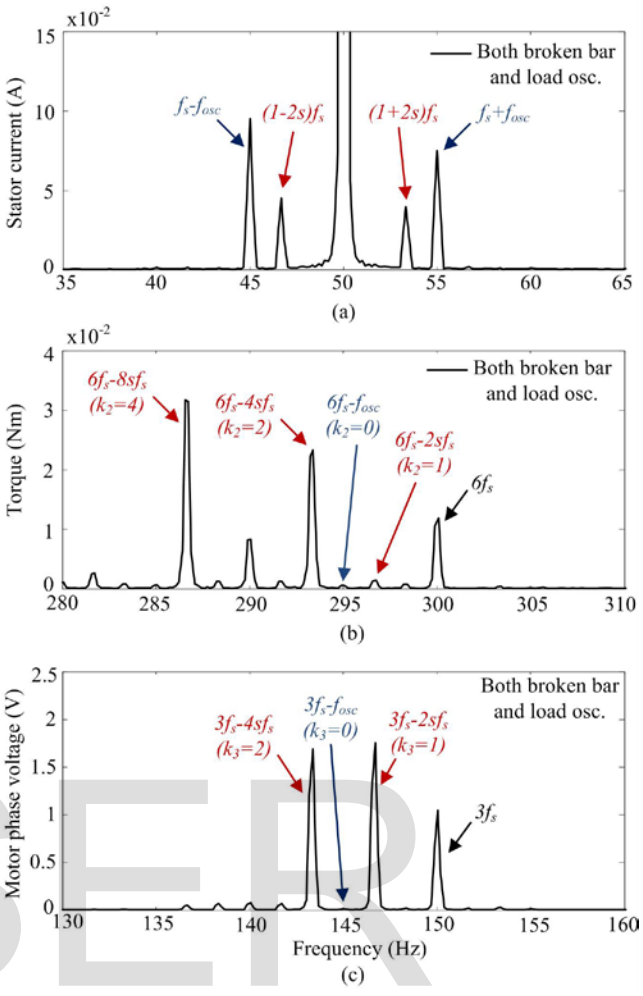

Fig. 6. Simulation results, 80% load, ($2sf_s$=3.3 Hz, f_{osc}=5 Hz) motor with both broken bar and load oscillation simultaneously
a) Stator current spectrum (35- 65 Hz)
b) Torque spectrum (280- 310 Hz)
c) Motor phase voltage spectrum (130- 160 Hz)

3 Simulation and Experimental Results

3.1 Simulation Results

For simulations, an integrated, multi-domain simulator; ANSYS Simplorer software is used and coupled with Maxwell software. By using Simplorer, all simulation data can transfer between the second or third party applications such as Maxwell, Matlab. Simulations are carried out to demonstrate that rotor bar failure and low frequency load torque oscillation can be separated from each other by using torque and motor phase voltage spectrum in line-fed star connected three phase induction motor. Load torque oscillation is modelled as given in (5) and two rotor bars are modified as broken in Maxwell simulation. Simulations are run for healthy rotor, broken rotor bar, load torque oscillation, and when both rotor fault and load torque oscillation exist simultaneously at full-load, 50 Hz supply frequency.

Fig. 5a. shows the spectrum of phase current when there are two broken rotor bars and low frequency load torque oscillation where motor speed is 1450 rpm and the motor slip is equal to 0.033. In order to prove the efficacy of the proposed approach, oscillation frequency is selected the same as broken bar fault signature frequency. Here, the sidebands harmonics of fundamental harmonic $(1\pm2s)f_s$ and $f_s\pm f_{osc}$ are clearly observed at 46.7 Hz and 53.3 Hz in the stator phase current spectrum. In the torque spectrum shown in Fig. 5b, around 6fs, the signatures related to broken bar fault $6f_s$-$2sf_s$, $6f_s$-$4sf_s$, $6f_s$-$8sf_s$ can clearly be seen whereas the sideband harmonics of 6fs frequency do not show up. It means that k_2 is equal to zero (Fig. 5b) as the separation harmonic (7) in load oscillation case. In addition, there is one more harmonic for broken bar case; $2sf_s$, and for load oscillation case; f_{osc}, which is close to dc component in torque spectrum. As shown in Fig. 5b, k_2 takes the integer values (k_2=1,2,4) during the broken bar fault for separation harmonic defined in (7). In Fig 5c., the presence of broken bars, sidebands of third harmonic $3f_s$-$2sf_s$ (k_3=1) and $3f_s$-$4sf_s$ (k_3=2) are observed in motor phase voltage spectrum. However, it is clearly seen in Fig. 5c. that there are no sidebands ($3f_s$-

f_{osc}) of $3f_s$ in the case of low frequency load torque oscillation ($k_3=0$).

In order to test the performance of separation harmonics, the simulations are run when two broken rotor bars and low frequency load torque oscillation exist simultaneously. Oscillation frequency f_{osc} is selected as 5 Hz which is different from broken bar frequency ($2sf_s=3.3$ Hz). As shown in Fig. 6a, oscillation ($f_s \pm f_{osc}$) and broken bar ($(1\pm 2s)f_s$) related harmonics are clearly seen in stator phase current spectrum at different frequencies. In Fig. 6b, broken bar related sideband harmonics ($6f_s$-$2sf_s$, $6f_s$-$4sf_s$, and ($6f_s$-$8sf_s$) are clear while oscillation related sideband harmonic ($6f_s$-f_{osc}) is not observed in torque spectrum.

The integer variable k_2 for the separation harmonic defined in (7) as: $k_2=1, 2, 4$ for broken bar fault condition, $k_2=0$ for load torque oscillation condition. Fig. 6c shows the motor phase voltage spectrum in the case of both broken bar fault and low frequency load oscillation. As seen in Fig. 6c, while broken bar related harmonics $3f_s$-$2sf_s$, $3f_s$-$4sf_s$ exist as the sidebands of $3f_s$, oscillation related harmonic $3f_s$-f_{osc} does not.

In order to examine broken bars location effects on the separation harmonics, three different cases are taken into account; case-a (Fig. 7a), case-b (Fig. 7b), and case-c (Fig. 7c). In all cases, the phase differences between the bars are in mechanically. Fig. 8 shows the torque and phase voltage spectrums in the case of broken bar fault. As shown in Fig. 8a (torque) and Fig. 8b (phase voltage) the amplitude of fault signatures are almost the same in case-a and case-b. In case-c it is observed that when the numbers of broken bars are increased, the amplitude of separation harmonics is increased. It is concluded that possible broken bars location does not affect the amplitude of separation harmonics defined in (7) and (9), -but number of broken bars do affect

It is noticed in the results that, even in healthy case there are some harmonics close to 6fs in torque spectrum. In this paper, the rotor has only one broken bar with three times less conductivity. In practice, the conductivity in the broken bar is equal to zero and hence, the fault signatures in torque spectrum are higher. It is well know that the amplitude of fault signatures is proportional to number of broken bars. If there are more broken bars in the rotor, the signatures appear remarkably in the torque spectrum.

3.1 Experimental Results

Identical induction motors are modified to test broken bar and load oscillation faults. A conventional test bed is used to extract the separation harmonics in induction motor. The experiments are implemented using a 2.2 kW three-phase, line-fed, star connected squirrel cage induction motor.

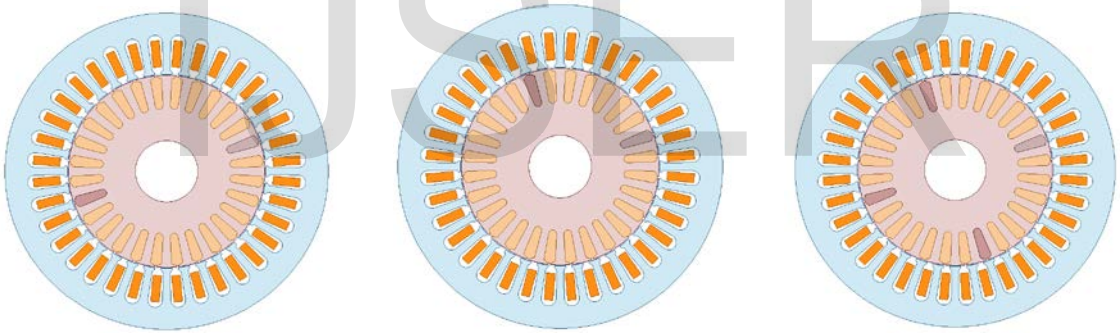

(a) case-*a* (b) case-*b* (c) case-*c*

Fig. 7. Case studies to show the broken bars location effects a) Two broken bars with 180° phase difference b) Two broken bars with 90° phase difference c) Four broken bars with 90° phase difference

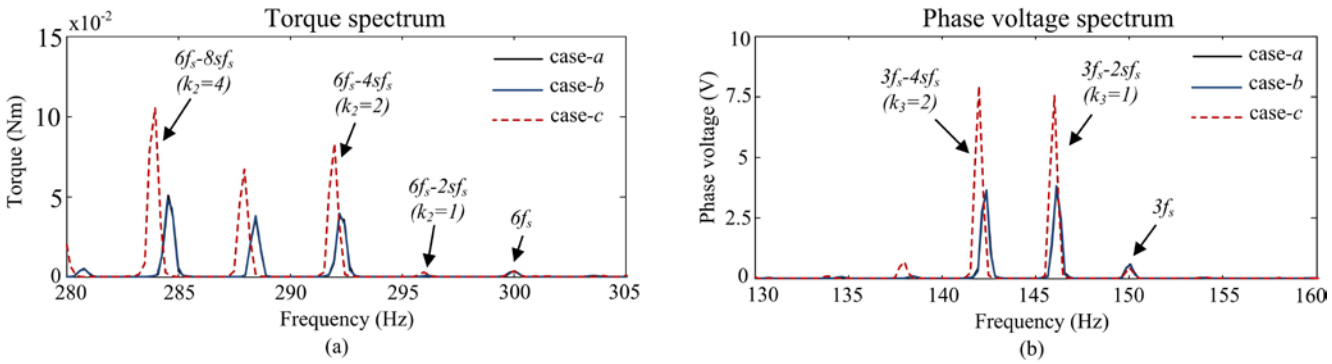

Fig. 8. Case studies, broken bar fault
a) Torque spectrum
b) Phase voltage spectrum

In order to verify the theoretical findings through simulations, the same motor parameters given in Table 1 are used. The test motor is loaded by a dc generator as shown in Fig. 11. A flexible coupling and laser alignment tool are used to have a perfect mechanical coupling. DC generator output is connected to resistor bank which means load can be set to desired value by switching the resistor bank. Hall-effect sensors and data acquisition card are used to sample phase currents and motor phase voltage respectively.

In order to generate a low frequency load torque oscillation at desired frequency, DC generator field windings are supplied with a constant DC voltage and modulated AC voltage at desired oscillating frequency. DC generator field voltage is provided through a variable DC source, signal generator (to change the desired frequency) and amplifier circuit (to increase the voltage level). Experiments are carried out in three different cases: two broken rotor bars without any oscillation, healthy rotor with load torque oscillation, and two broken rotor bars with load torque oscillation to show the effectiveness of proposed patterns.

Fig. 9a shows the stator current spectrum of motor with two broken bars and load oscillation under 80% load where supply frequency is 50 Hz. In this particular tests, the broken bar fault and load oscillation frequency is $2sf_s=f_{osc}=4.2$ *Hz*. Two sidebands harmonics; $(1\pm2s)f_s$ (for broken), are clearly seen at 45.8 Hz and 54.2 Hz in the stator phase current spectrum. The same sideband harmonics; $f_s\pm f_{osc}$ do exist when there is load oscillation as well. Therefore, analysing only stator phase current spectrum is not sufficient to determine whether these harmonics are related to broken bar or load oscillation. However, when the motor phase voltage spectrum around the $3f_s$ is analysed, load oscillation related sideband harmonics are not observed though broken bar related the sideband harmonics, $3f_s$-$2sf_s$ (k_3=1) and $3f_s$-$4sf_s$ (k_3=2), are as shown in Fig. 9b.

In the next test, load torque oscillation frequency is selected different than broken bar frequency to show the efficacy of separation harmonics. Oscillation ($f_s\pm f_{osc}$) and broken bar fault $(1\pm2s)f_s$ related sideband harmonics of fundamental component clearly appear in the stator current spectrum as shown in Fig. 10a. Oscillation and broken bar fault frequencies are at 6 Hz and 4.2 Hz respectively. When the motor phase voltage spectrum is analysed, only broken bar related sidebands harmonics $3f_s$-$2sf_s$, $3f_s$-$4sf_s$ are observed as show in Fig 10b. However, oscillation related sideband harmonic ($3f_s$-f_{osc}) in motor phase voltage spectrum do not appear.

In order to show the effects of load on the separation harmonics in torque and phase voltage spectrums, motor is run under different torque levels. As shown in Fig.12a, the harmonics at $6f_s$-$4sf_s$ and $6f_s$-$8sf_s$ increase almost linearly proportional to increasing torques. Fig. 12b. shows the behaviour of motor phase voltage harmonics with different torques. The harmonics at $3f_s$-$2sf_s$ and $3f_s$-$4sf_s$ linearly rise with motor load and $3f_s$-$2sf_s$ has always higher amplitude than harmonic at $3f_s$-$4sf_s$. After several simulations, the harmonic at $6f_s$-$8sf_s$ in torque spectrum is found to be the most reliable harmonic to separate broken bar fault from low frequency load torque oscillation. Moreover, the amplitudes of $6f_s$-$2sf_s$ and $6f_s$-$4sf_s$ in torque spectrum get higher with increasing number of broken bars. In phase voltage spectrum, $3f_s$-$2sf_s$ and $3f_s$-$4sf_s$ are very good indicators to separate broken bar faults from low frequency load torque oscillation.

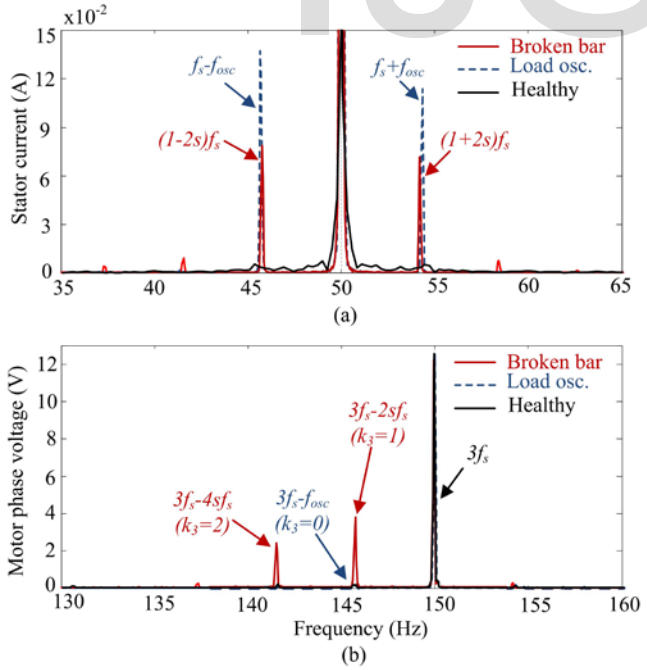

Fig. 9. Experimental results, 80% load, ($2sf_s= f_{osc}$ =4.2 Hz) broken bar (solid line), load oscillation (dashed line)
a) Stator current spectrum (35- 65 Hz)
b) Motor phase voltage spectrum (130- 160 Hz)

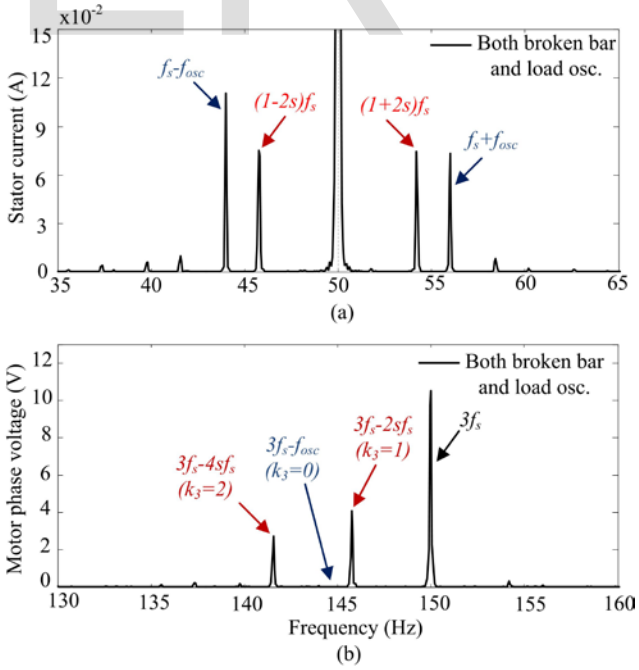

Fig. 10. Experimental results, 80% load, ($2sf_s$=4.2 Hz, f_{osc}=6 Hz) motor with both broken bars and load oscillation simultaneously
a) Stator current spectrum (35- 65 Hz)
b) Motor phase voltage spectrum (130- 160 Hz)

Fig. 11. Experimental setup
a) Induction motor
b) DC generator
c) Rotor with two broken bars
d) Amplifier circuit
e) Resistor bank
f) Signal generator

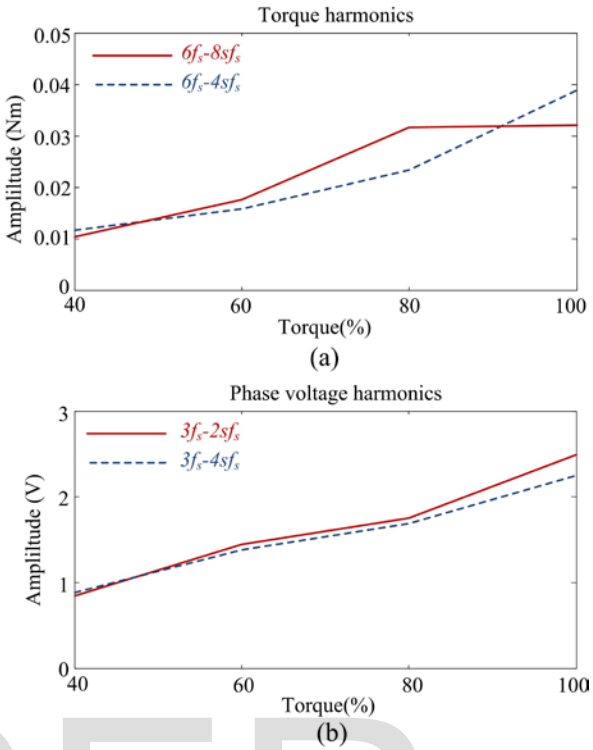

Fig. 12. The behaviour of separation harmonics
a) Torque harmonics
b) Phase voltage harmonics

Table. 2 shows the critical harmonics for different cases. As it is pointed out here, the harmonics $6f_s$-$2sf_s$, $6f_s$-$4sf_s$, and especially $6f_s$-$8sf_s$ (in the torque spectrum) and $3f_s$-$2sf_s$, $3f_s$-$4sf_s$ (in the motor phase voltage spectrum) are ideal indicators of broken bar failures.

TABLE 2
HARMONIC LISTS FOR DIFFERENT CASES

Harmonic	Torque		Motor phase voltage	
	Broken	Oscillation	Broken	Oscillation
$2sf_s$	✓	x	N/A	N/A
f_{osc}	x	✓	N/A	N/A
$6f_s - 2sf_s$	✓	x	N/A	N/A
$6f_s - 4sf_s$	✓	x	N/A	N/A
$6f_s - 8sf_s$	✓	x	N/A	N/A
$6f_s - f_{osc}$	x	x	N/A	N/A
$3f_s - 2sf_s$	N/A	N/A	✓	x
$3f_s - 4sf_s$	N/A	N/A	✓	x
$3f_s - f_{osc}$	N/A	N/A	x	x

4 CONCLUSION

In this paper, separation patterns have been presented to discern broken bar faults from low frequency load torque oscillation in star connected induction motors. The proposed separation signatures are defined in torque and motor phase voltage spectrums. The proposed patterns are verified through both simulation and experimental results. It is shown that the broken bar failure can be discerned from low frequency load torque oscillation by using the sidebands of $6f_s$ (torque spectrum) and the sidebands of $3f_s$ (motor phase voltage spectrum) in three-phase line-fed star connected induction motor. If harmonics $(6f_s\text{-}2k_2sf_s)$ appear on the sidebands of 6fs (for the torque spectrum) and the sidebands of $3f_s$ $(3f_s\text{-}2k_3sf_s)$ (for the motor phase voltage spectrum), it can be concluded that this is a broken bar condition without load oscillation. Results show that separation harmonics for both torque and motor phase voltage spectrum don't depend on load level and inertia. It is justified that the presented approach works reliably over the full speed and load range.

REFERENCES

[1] S. Nandi, H. A. Toliyat, L. Xiaodong, "Condition Monitoring and Fault Diagnosis of Electrical Motors—A Review," *IEEE Trans. Energy Convers.*, vol. 20, no. 4, pp. 719–729, 2005, doi: 10.1109/TEC.2005.847955

[2] G. B. Kliman, R.A. Koegl, J. Stein et al, "Noninvasive Detection of Broken Rotor Bars in Operating Induction Motors," *IEEE Trans. Energy Convers.*, vol. 3, no.4, pp. 873-879, 1988, doi: 10.1109/TEC.2005.847955

[3] X. Ying, "Performance Evaluation and Thermal Fields Analysis of Induction Motor with Broken Rotor Bars Located at Different Relative Positions," *Magnetics, IEEE Transactions on*, vol. 46, no.5, pp. 1243-1250, 2010

[4] J. Martinez, A. Belahcen, A. Arkkio, "Broken Bar Indicators for Cage Induction Motors and Their Relationship with the Number of Consecutive Broken Bars," *IET Electr. Power Appl.*, vol. 7, no. 8, pp. 633-642, 2013

[5] J. Faiz, B. M. Ebrahimi, "A New Pattern for Detecting Broken Rotor Bars in Induction Motors during Start-Up," *Magnetics, IEEE Transactions on*, vol. 44, no. 12, pp. 4673-4683, 2008

[6] M. Kang, J-M. Kim, "Reliable Fault Diagnosis of Multiple Induction Motor Defects Using A 2-D Representation of Shannon Wavelets," *Magnetics, IEEE Transactions on*, vol. 50, no. 10, pp. 1-13, 2014

[7] M. F. Cabanas, F. Pedrayes, M. R. Gonzalez, et al., "A New Electronic Instrument for The Early Detection of Broken Rotor Bars in Asynchronous Motors Working under Arbitrary Load Conditions," *Proc. Diagnostics for Electric Machines, Power Electronics and Drives, SDEMPED 2005, 5th IEEE International Symposium on* , pp. 8-16, 2005

[8] M. F Cabanas, F. Pedrayes, C. H. Rojas, et al., "A New Portable, Self-Powered, and Wireless Instrument for the Early Detection of Broken Rotor Bars in Induction Motors," *Industrial Electronics, IEEE Transactions on*, vol. 58, no. 10, pp. 4917-4930, 2011

[9] C. Kral, H. Kapeller, F. Pirker, G. Pascoli, "Discrimination of Rotor Faults and Low Frequency Load Torque Modulations of Squirrel Cage Induction Machines by means of the Vienna Monitoring Method," *Proc. Power Electronics Specialists Conference, PESC '05 IEEE 36th* , pp. 2861-2866, 2005

[10] G. Didier, E. Ternisien, H. Razik, "Detection of Incipient Rotor Cage Fault and Mechanical Abnormalities in Induction Motor Using Global Modulation Index on The Line Current Spectrum," *Proc. Diagnostics for Electric Machines, Power Electronics and Drives (SDEMPED)*, pp. 1-6, 2005

[11] C. H. Angelo, G. R. Bossio, G. O. Garcia, "Discriminating Broken Rotor Bar from Load Oscillation using Active and Reactive Powers Components," *IET Electr. Power Appl.*, vol. 4, no. 4, pp. 281-290, 2010

[12] G. R Bossio, De Angelo, C. H., Bossio, J. M., et al, "Separating Broken Rotor Bars and Load Oscillations on IM Fault Diagnosis through the Instantaneous Active and Reactive Currents," *IEEE Transactions on Industrial Electronics*, vol. 56, no. 11, pp. 4571-4580, 2009

[13] C. M. Pezzani, P. D. Donolo, A. M. Castellino, et al, "A New Approach to The Park's Vector For Broken Bars and Load Oscillation Diagnosis on IM," *Proc. Int. Conf. on Industrial Technology (ICIT)*, pp. 1221-1226, 2010

[14] C. Concari, G. Franceschini, C. Tassoni, "Induction Machine Current Space Vector Features to Effectively Discern and Quantify Rotor Faults and External Torque Ripple," *IET Electr. Power Appl.,* vol. 6, no. 6, pp. 310-321, 2012

[15] C. Concari, G. Franceschini, C. Tassoni, "Discerning Mechanical Load Unbalances From Rotor Faults in Induction Machines through Current Space Vector Components," *Proc. IECON 2010 - 36th Annual Conference on IEEE Industrial Electronics Society*, pp. 2609-2614, 2010

[16] C. Concari, G. Franceschini, C. Tassoni, "A MCSA Procedure to Diagnose Low Frequency Mechanical Unbalances in Induction Machines," *Proc. Electrical Machines (ICEM), 2010 XIX International Conference on*, pp. 1-6, 2010

[17] S. M. A. Cruz, "An Active-Reactive Power Method for the Diagnosis of Rotor Faults in Three-Phase Induction Motors Operating Under Time-Varying Load Conditions," *IEEE Transactions on Energy Con.*, vol. 27, no. 1, pp. 71-84, 2012

[18] Cruz Sergio, and Flavio Gaspar, "A New Method to Diagnose Rotor Faults in 3-Phase Induction Motors Coupled to Time-Varying Loads" *Przeglad Electrotechniczny*, 1a, pp. 202-206, 2012

[19] M. Drif, J. O. Estima, A. J. M. Cardoso, "Discriminating Rotor Cage Faults and Mechanical Load Oscillations in Three-Phase Induction Motors by the Stator Instantaneous Complex Apparent Impedance," *Proc. Energy Conversion Congress and Exposition (ECCE)*, pp. 3024-3031, 2012

[20] K. N Gyftakis, D. V. Spyropoulos, J.C. Kappatou, et al, "Taking Advantage of The Induction Motor Inherent Eccentricity Aiming to Discriminate the Broken Bar Fault from Load Oscillations," *Proc. International Conference on Electrical Machines (ICEM),* pp. 1933-1939, 2014

[21] M. Drif, A. J .M. Cardoso, "Discriminating the Simultaneous Occurrence of Three-Phase Induction Motor Rotor Faults and Mechanical Load Oscillations by the Instantaneous Active and Reactive Power Media Signature Analyses," *Industrial Electronics, IEEE Transactions on*, vol. 59, no. 3, pp. 1630-1639, 2012

[22] Maxwell Online Help, "ANSYS Electromagnetics Suite 15.0," 2013

[23] C. Hargis, B.g. Gaydon, and K. Kamish, "The Detection of Rotor Defects in Induction Motors," *Proc. Institutie Electrial Engineering EMDA Conf*, pp. 216-220, 1982

[24] G.B. Kliman, R.A. Koegl, J. Stein, R.D. Endicott, M.W. Madden, "Noninvasive Detection of Broken Rotor Bars in operating Induction Motors," *IEEE Transactions on Energy Conversion,* vol. 3, pp. 873-879, 1988.

[25] N.M. Elkasabgy, R. Anthony Eastham, Dawson, Graham E., "Detection of Broken Bars in The Cage Rotor on An Induction Machine," *Industry Applications, IEEE Transactions on* , vol. 28, no. 1, pp. 165-171, 1992

[26] L.Wu, "Separating Load Torque Oscillation and Rotor Faults in Stator Current Based-Induction Motor Condition Monitoring, " PhD dissertation, Georgia Institute of Technology, 2007

[27] K. N. Gyftakis, D.V. Spyropoulos, J. C. Kappatou, et al, "A Novel Approach for Broken Bar Fault Diagnosis in Induction Motors through Torque Monitoring," *IEEE Trans. Energy Convers.*, vol. 28, no. 2, pp. 267-277, 2013